Density-functional study of Fe_3Al: LSDA versus GGA

F. Lechermann, F. Welsch, C. Elsässer, C. Ederer, and M. Fähnle
Max-Planck-Institut für Metallforschung, Heisenbergstrasse 1, D-70569 Stuttgart, Germany

J. M. Sanchez
Texas Materials Institute, The University of Texas at Austin, Austin, Texas 78712

B. Meyer
Lehrstuhl für Theoretische Chemie, Ruhr-Universität Bochum, 44780 Bochum, Germany
(Received 12 December 2001; published 22 March 2002)

The local-spin-density approximation and the generalized-gradient approximation (GGA) are used to perform density-functional total-energy calculations at zero temperature for Fe_3Al in the ordered $D0_3$ and $L1_2$ structures. Our calculations show that commonly used GGA functionals fail to predict the experimentally stable $D0_3$ structure as the one with the lower total energy. This qualitative discrepancy with experiment is attributed to an overestimation of the magnetic energy in GGA. The calculations were carried out using the mixed-basis pseudopotential (MBPP) method in the frozen-core approximation and the full-potential linearized-augmented-plane-wave (FLAPW) method, both with and without spin polarization. Although there are small differences in the magnitudes of the magnetic moments and the magnetic energies obtained with MBPP and FLAPW, both methods yield the same qualitative result.

DOI: 10.1103/PhysRevB.65.132104 PACS number(s): 71.15.Mb, 71.15.Nc, 75.50.Bb

In the last decade it became clear that density-functional theory (DFT) in the local-spin-density approximation (LSDA) is able to describe the structural and magnetic properties of many materials in an appropriate manner. On the other hand, there are also systems for which this approximation yields erroneous results. One of the best-known examples is elementary Fe, for which LSDA predicts a nonmagnetic face-centered-cubic (fcc) structure to be energetically more favorable than the ferromagnetic (fm) body-centered-cubic (bcc) state which—however—is the real ground state of Fe in nature. This problem was solved (see, for instance, Ref. 1, and references therein) by replacing the LSDA with the generalized-gradient approximation (GGA), thereby stabilizing the fm bcc state. Later it turned out that the formation energy of a vacancy in Fe is drastically reduced when replacing LSDA by GGA whereas this replacement has only a minor influence on the vacancy formation energies of other transition metals.[2]

In this context it is essential to note that there is a significant difference between working within LSDA and working within GGA. Although there exist different analytical forms for both of the two approximations, there is nearly complete agreement about all the conditions that have to be fulfilled by the corresponding analytical representations only in the case of LSDA. Therefore, there are only minor differences in the existing LSDA functionals. As there is still no such general agreement concerning GGA, various GGA functionals can yield very different results.

The natural question investigated in this paper is whether the sensitivity of the results to the approximation used for the exchange-correlation functional (i.e., LSDA, GGA, and their different analytical representations) observed in elemental Fe is also evidenced in compounds involving Fe. In particular, we focus on the technologically important Fe-Al binary system and point out the inability of the GGA after Perdew, Burke, and Ernzerhof[3] (PBE) and the more sophisticated older version of this exchange-correlation functional after Perdew and Wang[4] (PW91) to predict the experimentally observed ground state for stoichiometric Fe_3Al.

The Al-rich part of the binary Fe-Al phase diagram exhibits rather complicated low-symmetry structures, while in the Fe-rich region the observed phases are the result of simple ordering on the bcc parent lattice. Starting from the equiatomic composition, a $B2$-FeAl phase extends prominently into the Fe-rich region. At approximately 67 at. % Fe, this dominant phase undergoes a low-temperature second-order transition into a $D0_3$-Fe_3Al phase. With increasing Fe concentration, the $D0_3$ phase transforms at around 77 at. % Fe via a first-order transition into a disordered bcc ($A2$) phase.

Although the initial difficulties encountered in describing bcc-Fe in DFT are satisfactorily resolved by GGA functionals, a more delicate problem concerning $B2$-FeAl still persists. For $B2$-FeAl, DFT calculations generally predict a ferromagnetic ground state for the ordered compound,[5] whereas experimentally, to our best knowledge, no net magnetic moment has been observed and $B2$-FeAl is generally classified as a Curie-Weiss-type paramagnet.[6] Thus, to our best knowledge, the correct experimental magnetic ground state for $B2$-FeAl is still an open question. A reason for the apparent discrepancy between experiment and the DFT results could be the fact that the magnetic state depends strongly on the degree of chemical order and, in ordered $B2$-FeAl, the different spin configurations, i.e., ferromagnetic, antiferromagnetic, spin spirals, and paramagnetic, are energetically very close.[7,8] Defects, which to a certain extent are always present in an experimental sample, could therefore have a strong influence on the observed magnetic state. On the other hand, Mohn *et al.*[9] showed in a recent work that by describing exchange and correlation within the local-density approximation $+U$ scheme[10] a nonmagnetic solution for ordered $B2$-FeAl is found for a certain range of U values. As the introduction of the Hubbard U normally enhances the ten-

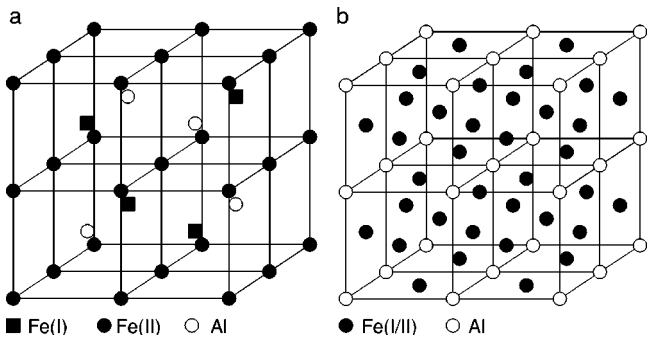

FIG. 1. (a) $D0_3$-Fe_3Al structure and (b) $L1_2$-Fe_3Al structure.

dencies towards magnetic order, this is an unusual result compared to other compounds.

The complexity of the magnetic behavior of the Fe-Al system can further be seen as the Fe concentration is increased from $B2$-FeAl towards the $D0_3$-Fe_3Al phase. For instance, magnetic measurements show[11] that $Fe_{0.7}Al_{0.3}$ becomes mictomagnetic below 92 K. At the stoichiometric composition, ordered $D0_3$-Fe_3Al is experimentally known[12] to exhibit ferromagnetic order.

The unit cell of the $D0_3$ structure [see Fig. 1(a)] can be described in terms of four fcc sublattices, three of which are occupied by the majority atoms (Fe) and the fourth by the minority atoms (Al). Of the three Fe sublattices, two are equivalent by symmetry and the atoms occupying them are commonly designated as Fe(II). The third, nonequivalent sublattice is occupied by so-called Fe(I) atoms. As can be seen in Fig. 1, all eight nearest neighbors of the Fe(I) sites are Fe atoms, whereas the Fe(II) sites are surrounded by four Fe and four Al nearest neighbors. Neutron-diffraction measurements[12] yield local magnetic moments of $\mu = 2.18\mu_B$ for Fe(I) and $\mu = 1.50\mu_B$ for Fe(II). Thus, as expected from the same nearest-neighbor environments, $\mu_{\mathrm{Fe(I)}}$ is very close to the magnetic moment of Fe in bcc-Fe ($2.22\mu_B$). According to Ref. 12 the Al moment should be zero.

In order to elucidate the energetics with respect to magnetism for Fe_3Al from the viewpoint of conventional DFT, we performed ground-state calculations for the $D0_3$ and the $L1_2$ structures with and without inclusion of collinear spin polarization. The $L1_2$ structure [see Fig. 1(b)] can be thought as the counterpart of the $D0_3$ structure on the fcc parent lattice, as it exhibits the same atom concentrations and it is also stabilized by strong near-neighbor interactions. In contrast to $D0_3$-Fe_3Al, all three Fe atoms in the simple cubic unit cell of the $L1_2$-Fe_3Al structure are equivalent by symmetry. Since one Fe atom has eight other Fe atoms and four Al atoms as nearest neighbors, we will refer to Fe atoms in the $L1_2$ structure as Fe(I/II) in order to distinguish them from those in the $D0_3$-Fe_3Al structure. The investigation of the $L1_2$ structure seems reasonable having in mind the series of intermetallic systems Ni-Al, Co-Al, and Fe-Al. All three of them exhibit an extended $B2$ phase near the equiatomic region. In Ni-Al there is a martensitic transformation via an orthorhombic Ni_5Al_3 phase to the $L1_2$-Ni_3Al phase. $B2$-CoAl transforms directly via a first-order transition with

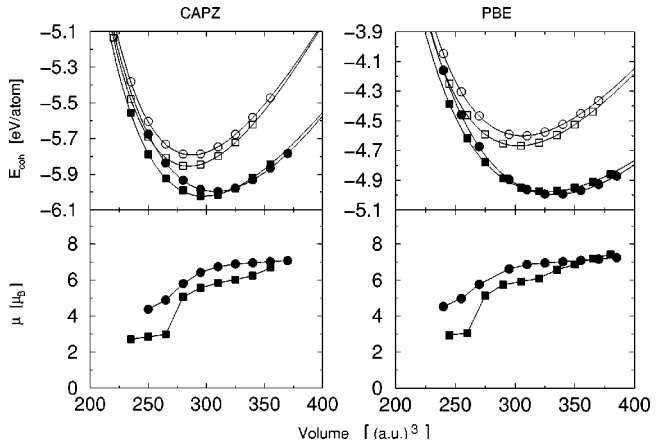

FIG. 2. Cohesive energy E_{coh} per atom and magnetic moment μ per unit cell within LSDA after CAPZ and GGA after PBE, according to the pseudopotential calculations. Squares indicate the $D0_3$ structure, circles the $L1_2$ structure. Open symbols belong to the spin-unpolarized calculations, filled symbols to the spin-polarized calculations, respectively.

increasing Co concentration into hcp-Co at low temperatures. Thus only in the Fe-Al system the bcc parent lattice remains stable in the whole transition-metal-rich region.

The main result of our calculations is that there is a qualitative discrepancy between LSDA and the used GGA functionals in describing the phase stability of Fe_3Al. Whereas LSDA yields the correct hierarchy, i.e., $D0_3$ is stable and $L1_2$ is metastable, GGA-PBE and GGA-PW91 predict $L1_2$ with a lower total energy and, therefore, yield the wrong ground state compared to experiment. Although according to our calculations the magnitude of the relevant total-energy difference does not exceed 50 meV/atom, this difference is nevertheless significant.

The relevant ground-state properties were determined by the *ab initio* pseudopotential method[13] with norm-conserving pseudopotentials for the elements Fe and Al including nonlinear core correction. The $3p$ semicore states for Fe were treated as valence states, since the frozen-core approximation for this shell is probably inadequate in this case.[14] The same exchange-correlation functional, i.e., either LSDA or GGA, was used for both the construction of the pseudopotentials and the subsequent crystal calculation. For each pseudopotential, relativistic effects were included in the scalar approximation, thereby modifying only the exchange part of the exchange-correlation functional. The mixed-basis set for the crystal calculations involved plane waves and nonoverlapping localized p and d orbitals for Fe.[15] For the exchange-correlation functional in LSDA we used the correlation of Ceperley and Alder,[16] as parametrized by Perdew and Zunger[17] (CAPZ). As already mentioned we used for the GGA calculations the representation of Perdew, Burke, and Ernzerhof[3] (PBE). However, in order to see the influence of the analytical representation of the exchange-correlation functional, we also performed calculations using different versions of the LSDA and GGA functionals. For LSDA we used, in addition to CAPZ, the correlation of Ceperley and Alder,[16] as parametrized by Vosko, Wilk, and Nusair.[18] Al-

TABLE I. Computed structural data within the mixed-basis pseudopotential (MBPP) and full-potential linearized-augmented-plane-wave (FLAPW) method. Spin-polarized calculations are indicated by ''sp,'' spin-unpolarized by ''up.'' The given difference between the total energies in both schemes for a given structure can be interpreted as the respective magnetic energy.

Method	Structure	a_{eq} (Å)	B (Mbar)	m_{tot} (μ_B)	$m_{Fe(I)}$ (μ_B)	$m_{Fe(I/II)}$ (μ_B)	$m_{Fe(II)}$ (μ_B)	m_{Al} (μ_B)	$E_{tot}^{D0_3\text{-sp}}-E_{tot}^{D0_3\text{-up}}$ (meV/atom)	$E_{tot}^{L1_2\text{-sp}}-E_{tot}^{L1_2\text{-up}}$ (meV/atom)	$E_{tot}^{D0_3}-E_{tot}^{L1_2}$ (meV/atom)
MBPP-CAPZ-up	$D0_3$	2.764	2.591								
	$L1_2$	3.493	2.531								−63.0
MBPP-CAPZ-sp	$D0_3$	2.806	1.920	5.67	2.33		1.76	−0.07	−167.2	−204.0	
	$L1_2$	3.573	1.900	6.70		2.28		−0.09			−26.2
MBPP-PBE-up	$D0_3$	2.821	2.181								
	$L1_2$	3.567	2.137								−68.2
MBPP-PBE-sp	$D0_3$	2.892	1.510	6.35	2.45		2.12	−0.13	−307.1	−396.3	
	$L1_2$	3.669	1.680	6.99		2.43		−0.16			21.0
FLAPW-PW92-up	$D0_3$	2.748	2.630								
	$L1_2$	3.473	2.569								−65.9
FLAPW-PW92-sp	$D0_3$	2.787	2.094	5.04	2.14		1.50	−0.04	−117.6	−140.4	
	$L1_2$	3.547	1.769	6.35		2.09		−0.05			−43.2
FLAPW-PBE-up	$D0_3$	2.807	2.207								
	$L1_2$	3.550	2.168								−70.5
FLAPW-PBE-sp	$D0_3$	2.869	1.693	5.95	2.39		1.90	−0.07	−240.7	−316.4	
	$L1_2$	3.651	1.749	6.91		2.33		−0.08			5.3
Experiment	$D0_3$	2.896[a]		5.60[b]	2.18[c]		1.50[c]				
					2.12[d]		1.46[d]				

[a]Reference 22.
[b]Reference 23.
[c]Determined by neutron diffraction (Ref. 12).
[d]Determined by Mössbauer spectroscopy (Ref. 24).

though this representation uses a slightly different spin interpolation formula for the correlation part than that used in CAPZ, the results showed only minor differences. Also, the replacement of PBE by the older functional of Perdew and Wang[4] from 1991 (PW91) yielded only marginally different results compared to PBE. This was expected, as these two GGA functionals are very similar. The Brillouin-zone integrations were carried out using 110 and 120 **k** points in the irreducible wedge for, respectively, the $D0_3$ and $L1_2$ structures. To perform these integrations, a Gaussian broadening with a width of 0.05 eV was used. The cutoff energy for the plane waves in the mixed-basis set was chosen to be $E_{PW}=24$ Ry. Increasing E_{PW} up to 48 Ry shows that relevant total-energy differences converging to better than 0.5 meV/atom can be obtained with $E_{PW}=24$ Ry. In order to ensure that our results are not significantly affected by the frozen-core approximation made in the pseudopotential calculations, we also performed the same calculations using the full-potential linearized-augmented-plane-wave (FLAPW) method. We used the WIEN97 code[19] with a chosen radius of the muffin-tin spheres R_{MT} of 2.0 a.u. and a plane-wave cutoff of $R_{MT}\times K_{max}=10.0$. The number of **k** points in the irreducible wedge of the Brillouin zone was 120 for both structures. In LSDA, we used the exchange-correlation functional of Perdew and Wang[20] (PW92) and in GGA we employed the PBE functional also used in the pseudopotential calculations.

In Fig. 2 we show the cohesive energy plotted as a function of the volume of the unit cell for the LSDA-CAPZ and the GGA-PBE functional, together with the magnetic moments per unit cell for the spin-polarized pseudopotential calculations. The solid lines for the cohesive energy are the result of a fit to a Murnaghan equation of state.[21] The equilibrium lattice constants and bulk moduli were determined from these fitted curves. The values are given in Table I along with the corresponding values obtained in the FLAPW calculations and the available experimental data for $D0_3$-Fe_3Al. Not surprisingly, the GGA-PBE functional gives a larger value for the equilibrium lattice constant of the $D0_3$ structure compared to the LSDA functionals, as it is well known that in most cases the frequent overbinding for transition metals and their compounds in LSDA is corrected with GGA. As already mentioned, with spin polarization the used GGA functionals yield the wrong ground state. Within the pseudopotential calculations, the total energy of $L1_2$-Fe_3Al is lower than that of $D0_3$-Fe_3Al by 21.0 meV/atom for the PBE functional, whereas LSDA-CAPZ correctly favors the $D0_3$ structure by 26.2 meV/atom. This qualitative difference between LSDA and the used GGA functionals is confirmed by the FLAPW calculations, although the difference in total energy for the two structures within spin-polarized GGA-PBE is smaller (5.3 meV/atom). In principle, due to the smallness of the latter value, there exists the possibility that $D0_3$ is only stabilized by phononic contributions to the free energy and that there is a transition to $L1_2$ at very low temperatures, thereby suggesting that the GGA functionals yield the correct description. However,

though common experimental phase diagram investigations do not cover such low temperatures, magnetic[23] and resistivity[25] measurements at temperatures as low as 2 K did not indicate an occurrence of $L1_2$-Fe_3Al.

The different results concerning stability within the spin-polarized and spin-unpolarized calculations suggest that the origin of the failure of GGA-PBE and GGA-PW91 to reproduce the correct hierarchy lies in the description of magnetism for this composition in the Fe-Al system. In Table I, the total magnetic moments and the site-resolved magnetic moments are given along with the total-energy differences between the spin-polarized and spin-unpolarized calculations for each structure. The local magnetic moments were determined by filling the whole crystal with nonoverlapping, touching spheres of the same size placed at each lattice point and computing the magnetic moment within the spheres. First, we note that the total and local moments obtained with the pseudopotential method are slightly bigger than the ones obtained with the FLAPW method. Since there is no experimental information about $L1_2$-Fe_3Al we cannot compare our values for the Fe(I/II) moment with measured data. Nevertheless, the calculated values are, for all cases, between the values of the Fe(I) and Fe(II) moments in $D0_3$-Fe_3Al, as is expected from the nearest-neighbor environments. We also want to note that in all cases the Al atoms couple antiferromagnetically to the Fe atoms with a magnitude of the order of $0.1\mu_B$, a result which is consistent with other calculations.[26,27]

Concentrating on the Fe moments it can be generally stated that the moments obtained by the LSDA are significantly smaller than those obtained by the GGA-PBE, and in the case of $D0_3$-Fe_3Al they are therefore in better agreement with the experimental values. Also, the energy gained upon magnetization is bigger in the GGA calculations (see Table I). It was already pointed out by Singh and Ashkenazi[28] that in GGA there is an increased tendency towards magnetism in general and, in particular, towards larger magnetic energies for magnetic materials. These authors suspect that GGA might be less reliable for magnetic than for nonmagnetic systems, because of the absence of further exact relations needed in the construction of GGA for spin-polarized systems, where there are more degrees of freedom. Thus it seems that an overestimation of the magnetic energy in GGA, which in other cases may just result in a small quantitative error, is shifting the $L1_2$ structure energetically below the $D0_3$ structure in the case of Fe_3Al resulting in a qualitatively wrong description of the ground state. Therefore it appears that neither LSDA, because of the wrong description of bcc-Fe, nor GGA, at least in the form of PBE or PW91, are capable of describing the Fe-Al phase diagram in a way consistent with experiment.

We note that *ab initio* calculations for Fe_3Al in the $D0_3$ and $L1_2$ structures have been previously reported by Watson and Weinert.[29] These authors, who employ the full-potential linearized augmented Slater-type orbital method (FLASTO) in LSDA, indicate that they find the ground state of the $L1_2$ structure to be nonmagnetic, which is in apparent disagreement with our results.

In summary, we have shown that the GGA fails to reproduce the experimental ground state in Fe_3Al for two of the most commonly used representations in solid-state calculations, i.e., PBE and PW91. Since, in contrast to LSDA, there is no general recipe for the construction of the GGA functional, and due to the smallness of the total-energy differences, we cannot exclude that there might exist other GGA representations which do not suffer from this inadequacy. Nevertheless, the difficulties encountered previously in the $B2$-FeAl compound and the results reported here for Fe_3Al seem to indicate that in the Fe-Al system one reaches the limit of accuracy of modern density-functional theory.

F. Lechermann was supported by a HSPIII doctoral scholarship from the Deutscher Akademischer Austauschdienst. Part of this work was also funded by the Deutsche Forschungsgemeinschaft.

[1] C. Elsässer *et al.*, J. Phys.: Condens. Matter **10**, 5081 (1998).
[2] P. Söderlind *et al.*, Phys. Rev. B **61**, 2579 (2000).
[3] J. P. Perdew *et al.*, Phys. Rev. Lett. **77**, 3865 (1996); **78**, 1396 (1997).
[4] J. P. Perdew, in *Electronic Structure of Solids '91*, edited by P. Ziesche and H. Eschrig (Akademie, Berlin, 1991).
[5] B. I. Min *et al.*, J. Magn. Magn. Mater. **54-57**, 1091 (1986).
[6] K. Miyatani and S. Iida, J. Phys. Soc. Jpn. **25**, 1008 (1968).
[7] V. L. Moruzzi and P. M. Marcus, Phys. Rev. B **47**, 7878 (1993).
[8] J. Bogner *et al.*, Phys. Rev. B **58**, 14 922 (1998).
[9] P. Mohn *et al.*, Phys. Rev. Lett. **87**, 196401 (2001).
[10] V. I. Anisimov *et al.*, Phys. Rev. B **44**, 943 (1991).
[11] R. D. Shull *et al.*, Solid State Commun. **20**, 863 (1976).
[12] S. J. Pickart and R. Nathans, Phys. Rev. **123**, 1163 (1961).
[13] D. Vanderbilt, Phys. Rev. B **32**, 8412 (1985).
[14] E. G. Moroni *et al.*, Phys. Rev. B **56**, 15 629 (1997).
[15] B. Meyer *et al.*, computer code FORTRAN 90, Program for Mixed-Basis-Pseudopotential Calculations for Crystals, Max-Planck-Institut für Metallforschung, Stuttgart.
[16] D. M. Ceperley and B. J. Alder, Phys. Rev. Lett. **45**, 566 (1980).
[17] J. P. Perdew and A. Zunger, Phys. Rev. B **23**, 5048 (1981).
[18] S. H. Vosko *et al.*, Can. J. Phys. **58**, 1200 (1980); S. H. Vosko and L. Wilk, Phys. Rev. B **22**, 3812 (1980).
[19] P. Blaha *et al.*, computer code WIEN97, Vienna University of Technology, Vienna, 1997.
[20] J. P. Perdew and Y. Wang, Phys. Rev. B **45**, 13 244 (1992).
[21] F. D. Murnaghan, Proc. Natl. Acad. Sci. U.S.A. **3**, 244 (1944).
[22] W. B. Pearson, *A Handbook of Lattice Spacings and Structures of Metals and Alloys* (Pergamon, Oxford, 1958).
[23] T. Wakiyama, J. Phys. Soc. Jpn. **32**, 1222 (1972).
[24] D. Satula *et al.*, J. Magn. Magn. Mater. **151**, 211 (1995).
[25] Y. Nishino *et al.*, Phys. Rev. Lett. **79**, 1909 (1997).
[26] O. Eriksson *et al.*, Phys. Rev. B **41**, 11 807 (1990).
[27] G. Y. Guo *et al.*, J. Phys.: Condens. Matter **10**, L119 (1998).
[28] D. J. Singh and J. Ashkenazi, Phys. Rev. B **46**, 11 570 (1993).
[29] R. E. Watson and M. Weinert, Phys. Rev. B **58**, 5981 (1998).